Numerical Study of Shock-Induced Combustion in a Hypersonic Non-uniformly Premixed Hydrogen/Air Flow

Iwata, K., Nakaya, S., Tsue, M.
Department of Aeronautics and Astronautics, the University of Tokyo
Bunkyo-ku, Tokyo, Japan

1 Introduction

Oblique detonation has been attracting increasing attention because of its potential for application to Oblique Detonation Wave Engine (ODWE) [1-3]. ODWE achieves premixing by injecting fuel upstream of the combustor, in the inlet or on the engine forebody. Premixed combustible mixture is ignited behind the shock front formed on a solid surface such as a sharp wedge or a blunted cylindrical body, thus creating oblique detonation or shock-induced combustion [4-6]. Previous works proved that ODWE can be comparable to Scramjet engine, which is a leading candidate for the hypersonic air-breathing propulsion system of a reusable SSTO space plane [7], in thrust coefficient around a flight Mach number of 11 [8], and can even be superior in specific thrust around and over a flight Mach number of 15 [9]. It is due to the fact that oblique detonation needs a shorter distance to complete combustion, which makes it possible to reduce the weight of the engine and alleviate the burden of cooling [1-3].

Such an innovative propulsion system motivated a lot of researchers to conduct extensive studies on the fundamental physics of oblique detonation and shock-induced combustion [4-6, 8-11]. Almost all of the previous works are limited to the conditions of perfectly premixed flow.

Since incomplete mixing is inevitable in ODWE, extensive studies on oblique detonation under non-uniform flow conditions are needed to understand a realistic phenomenon in the combustor. However, studies on such phenomena are scarce and comprehensive discussion has not been done yet [12, 13].

This study then aims to investigate structures of oblique detonation and shock-induced combustion under non-uniformly premixed conditions through a parametric numerical study with variable fuel concentration gradients, and to discuss the influential factors in their newly observed structures.

2 Numerical Methods

Axisymmetric two-dimensional laminar Navie-Stokes equations were solved including 9 species transport equations (N_2, H_2, O_2, OH, H_2O, H, O, HO_2, H_2O_2), whose chemical source terms were evaluated according to Arrhenius's law with Konnov's detailed chemical kinetic mechanism consisting of 27 elementary reactions [14]. Convection terms were discretized using Harten-Yee's upwind TVD scheme [15]. Diffusive terms were discretized with the second-order central difference.

Both steady and unsteady structures were observed in this study. Second-order Runge-Kutta method [16] was used for the unsteady cases, while fully implicit scheme with LU-SGS [17] and Point Implicit Mehod [18] combined for the steady cases.

Correspondence to: 3138826900@mail.ecc.u-tokyo.ac.jp

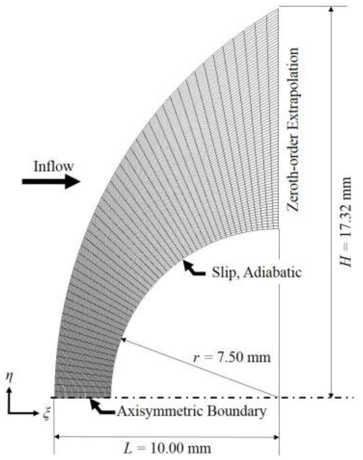

Figure 1. Computational grid used in the present study (every-tenth grid lines are shown).

The computational grid is illustrated in Figure 1. ξ=ξ_{max} line corresponds to the surface of the spherical projectile. The domain contains only one side of the axis for the axisymmetric assumption which is justified by the previous experimental works [11, 19]. We exclude the wake region for the sake of lower computational costs and direct comparison with abundance of the previous works on the frontal phenomena. The number of grids is 750 (ξ) × 500 (η) which was proved to show little grid dependency by the preliminary computations. This grid does not fully resolve all the waves present in the detonation structures, but enables us to discuss their general structures which are our greatest concern.
Slip and adiabatic wall condition is adopted on the spherical surface which was validated by another preliminary computation showing that a boundary layer has only negligible effects. Zero-gradient extrapolation is used on the outlet boundary.
Incoming condition of the mixture for the uniformly premixed case was referred from one of Lehr's experiments [19] where stoichiometric hydrogen-air mixture approaches a hypersonic projectile at a Mach number of 6.46, a static temperature of 292 K, and a static pressure of 43,383 Pa.
Inlet hydrogen distributions were introduced into the above condition described by the Gaussian function as shown in the equation below, which is justified by the measurements of fuel distributions in the previous works where concentration decreases exponentially away from the centerline[4, 5].

$$X_{\mathrm{H_2,inlet}} = X_{\mathrm{H_2,centerline}} \exp\left(-ay^2\right)$$

$X_{\mathrm{H_2,centerline}}$ and a denote variables specific for each case, which were arranged so that total equivalence ratio in y=0~y_s (the location of the shock front at the outlet in the uniform case) be unity. ϕ_{max} (on the centerline), ϕ_{min} (at y=y_s) resulting from the two variables chosen are listed in Table 1. Velocity, a static temperature, a static pressure remained constant in the whole region for all the cases.
The numerical method described above were validated against the two experimental cases conducted by Lehr [19], namely, the presently referred uniform case which created a smooth-front oblique detonation on a spherical projectile, and the case at a Mach number of 5.03 which created an oscillating mode of shock-induced combustion. The locations of the shock and flame front, frequency of oscillating phenomenon were well resolved.

Table 1: The values of non-uniformity parameters

Case	ϕ_{max}	ϕ_{min}	ϕ_{total}
1	1.50	0.67	1.00
2	2.25	0.46	1.00
3	3.50	0.32	1.00
4	5.00	0.25	1.00
5	7.00	0.20	1.00

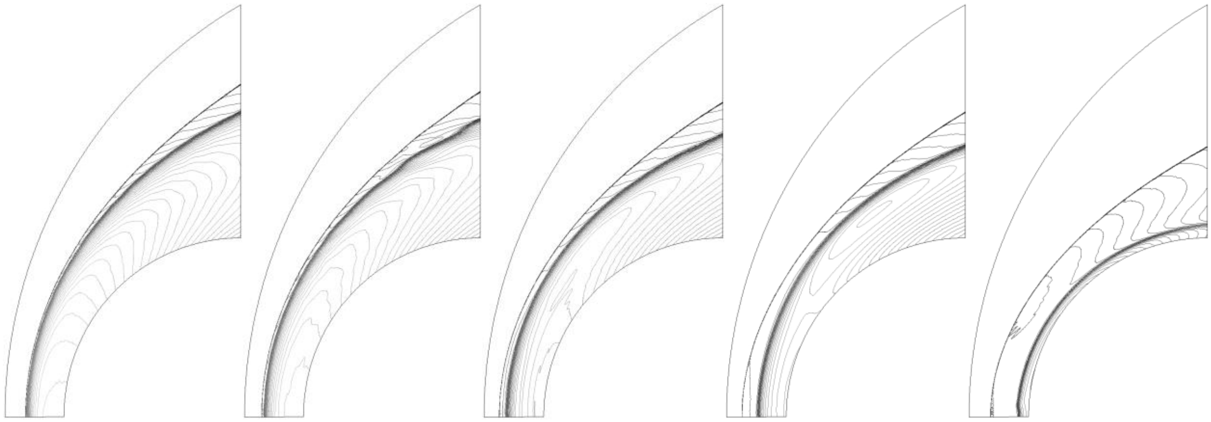

(a) Case 1 (b) Case 2 (c) Case 3 (d) Case 4 (e) Case 5

Figure 2. Instantaneous temperature contours of the non-uniform cases; the increment is 50 K.

3 Smooth-Front Oblique Detonation (Case 1)

Oblique detonation/shock-induced combustion generated by the non-uniform concentrations listed in Table 1 are displayed in Figure 2 as instantaneous temperature contours.

Smooth-front oblique detonation was observed in Case 1 (Figure 2(a)). The shock stand off disctance increased, and the radial position of the shock and flame at the outlet boundary decreased from those of the uniformly premixed one. The previous workers observed the same tendency, attributing it to an incoming Mach number variation [12, 13]. In order to verify their arguments, another computation was performed with inlet velocity distribution giving the same Mach number gradient as that of Case 1, but with entirely stoichiometric composition. It also resulted in a smooth-front oblique detonation with the same front positions. The result reconfirms that Mach number is a determinant factor.

In order to extract and discuss the influences of a reactivity variation, another method based on zero-dimensional numerical simulation was taken which solves Rankin-Hugoniot [20] relations to calculate the post-shock condition using the shock angles obtained from the two-dimesnional result, and then numerically simulates isochoric zero-dimensional combustion. Stoichiometric 0D simulation was also carried out in which the post-shock composition is replaced by stoichiometric mixture.

Resulting induction length distributions from the two-dimensional and 0D simulations are illustrated in Figure 3. Close agreement is seen between the two-dimensional and 0D results in $\eta < 370$, ascertaining the validity of zero-dimensional analysis. Large difference in $\eta > 370$ is caused by the two-dimensionality. One important point to note is that there is no difference between stoichiometric 0D and normal 0D result. This fact confirms that a reactivity distribution has a negligible influence.

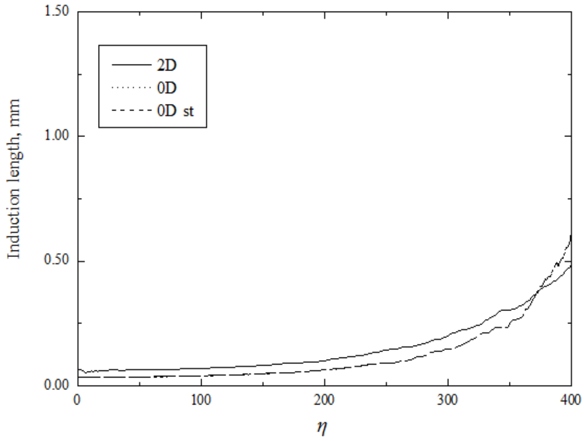

Figure 3. Induction length profile of Case 1 with the result of 0D simulations

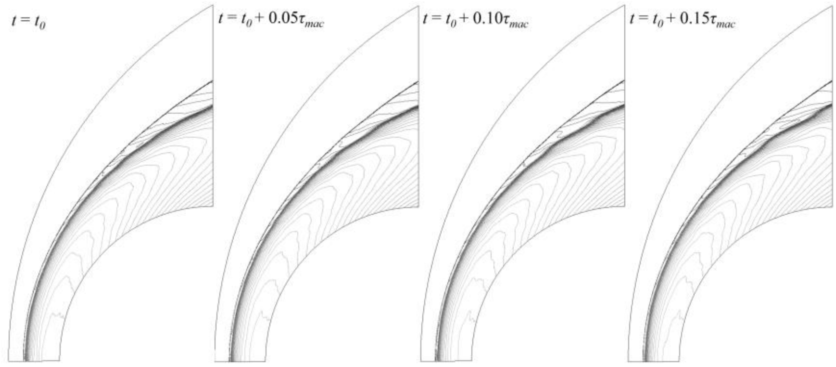

Figure 4. Time history of temperature contours in a part of one period of oscillation in Case 2

4 Unsteady Shock-Induced Combustion (Case2, 3)

Unsteady oscillating shock-induced combustion occurred in Case 2 and Case 3. Amplitude and wavelength of the oscillating flame front in Case 2 (Figure 2(b)) increase outward. Strong unsteadiness is solely seen in the outer region. On the contrary, those in Case 3 decreases outward and the inner region solely exhibits an unsteady phenomenon. Their behaviors are totally different from that seen in the oscillating shock-induced combustion in a uniform mixture [21].

A time history of temperature contours in a part of an oscillation period seen in Case 2 are displayed in Figure 4. t_o denotes a starting time of the time history. τ_{mac} = 14.96 μs is one period of the macroscopic unsteady phenomenon. Amplification of the wavy structures appearing in the outer region alternates between the stronger and weaker one in one period. Figure 4 corresponds to a part of the history of the stronger one. It can be seen that two corrugated waves are transmitted downstream with their amplitude and wavelength becoming larger. After passing the outlet boundary, amplification becomes so weak that no apparent corrugation appears (the weaker period). However, amplification subsequently recovers and the stronger period returns.

Transmission of the waves is observed to originate on the centerline where the shock and flame fronts send a compression wave or contact discontinuity to each other to oscillate, as the uniform cases experience [21, 22]. Non-uniform corrugated structures on the other hand can be attributed to variation of normal-shock ignition delay time in the post shock region. Thorough analyses by the previous workers have revealed that a characteristic length of the corrugated structure is linearly dependent on the ignition delay time behind the normal component of the shock front [21, 22]. Normal-shock ignition delay time according to the definition above is uniform in the whole region in the cases of a uniformly premixed mixture, but it is not true in the non-uniform cases considered in the present study, leading to non-uniformity in the shapes of the corrugation outward.

5 Steady Shock-Induced Combustion (Case 4, 5)

Steady shock-induced combustion were observed in Case 4 and Case 5 (Figure 2(d), (e)). The shock and flame fronts are no longer close to each other enough to make a visible interaction. One unique feature of the flame front in Case 4 is that the minimum induction length is located outside the centerline (the outer minimum induction length), distinctly differently from the uniform case where induction length increases monotonously toward the outer region. Case 5 on the contrary encounters the minimum in the central region as uniform conditions do.

Induction distributions in both cases with 0D results are illustrated in Figure 5. The minimum location in Case 5 (Figure 5(a)) is along η = 270 line. The outer minimum induction length is reproduced by 0D simulations, but deviation is larger than that seen in Figure 3 for Case 1. This is more evident in Case 5 (Figure 5(b)), still predicting the outer minimum induction which is not consistent with the two-dimensional result. Those deviations indicate two-dimensionality has a larger influence. Another 0D simulation taking into account velocity variation along streamlines was then conducted (Streamline simulation) to make clear two-dimensional effects, the results of which are plotted in the same figures.

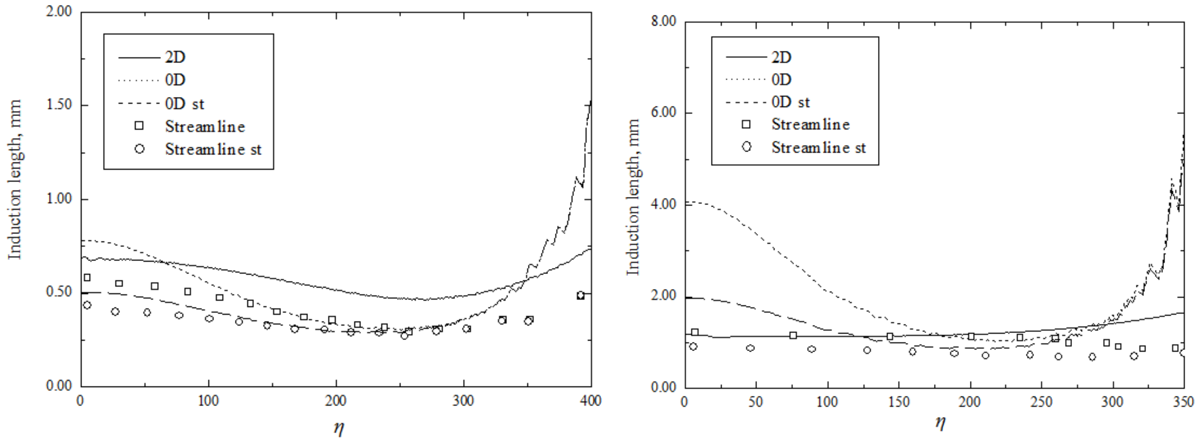

(a) Case 4 (b) Case 5

Figure 5. Induction length profile of Case 4 and Case 5 with the result of 0D simulations

Streamline simulation cannot meaningfully reduce the error in Case 4 (Figure 5(a)), but qualitative tendency of induction length including the minimum location is almost perfectly reproduced. Induction length tendency is also well predicted by Streamline simulation in Case 5 (Figure 5(b)) especially in the inner region, although the outer region still exhibits deviation due to improperness of the isochoric assumption. Another point to note for Figure 5(a) is that variable concentration simulations and entirely stoichiometric ones make clearer differences than observed in Figure 3 for Case 1. This fact indicates that a reactivity variation is strongly influential on the structure of steady shock-induced combustion observed in the present study. Smaller difference between the results of 0D simulations and Streamline simulations here indicates a smaller influence of two-dimensionality of the post-shock flow. The two variations of streamline simulations in Case 5 on the other hand make a smaller difference, compared with the difference between the results of 0D simulations and Streamline ones. It indicates that two-dimensional post-shock flow field exerts a larger influence in Case 5, rather than a reactivity variation.

6 Conclusion

Oblique detonation and shock-induced combustion formed on a hypersonic projectile under non-uniformly premixed conditions were numerically investigated through a parametric study with variable concentration gradients. Inlet hydrogen distributions were described by the Gaussian function, arranged to keep total equivalence ratio in the whole region unity.

As non-uniformity increased, oblique detonation experienced deformation (Case 1, ϕ_{max} = 1.50), then the shock and flame front decoupled into oscillating shock-induced combustion (Case 2, 3, ϕ_{max} =2.25, 3.50), and transformed into steady shock-induced combustion (Case 4, 5, ϕ_{max} =5.00, 7.00).

Unsteady shock-induced combustion observed in Case 2 and 3 exhibits the unique features in which amplitude of oscillation increases or decreases toward the outer region. Steady shock-induced combustion observed in Case 4 experienced the minimum induction length far outside the centerline.

Influential factors determining the above non-uniformly premixed structures also changed. Mach number variation has the largest influence on the structure of oblique detonation in Case 1. However, a reactivity variation also strongly influences the steady structure in Case 4. Even steeper conditions made the two-dimensional post-shock field the most dominant in controlling the structure in Case 5.

Future works will be needed to investigate non-uniform phenomena on straight shaped cones/wedges for availability of a simplified theoretical analysis. Unstable oblique detonation with transverse wave structure will also be surveyed. Extension to the wake of the projectile will be also needed to investigate reacting behaviors of unburned fuels, which may reveal another unique flame structure.

References

[1] Dunlap R et al. (1958). A Preliminary Study of the Application of Steady-State Detonative Combustion to a Reaction Engine. Jet. Prop. 28, 7: 451-456.

[2] Wolanski P (2013). Detonative Propulsion. Proc. Combust. Inst. 34: 125-158.

[3] Wei H et al. (2010). Research status of key techniques for shock-induced combustion ramjet (shcramjet) engine. Sci. China Tech. Sci. 53, 1: 220-226.

[4] Gross RA. (1960). A Study of Supersonic Combustion. J. Aero. Sci. 27, 7: 517-524.

[5] Menees GP et al. (1991). Analytical and Experimental Investigations of the Oblique Detonation Wave Engine Concept. NASA TM 102839.

[6] Ess PR et al. (1973). Blunt-Body Generated Detonation in Viscous Hypersonic Ducted Flows. J. Prop. Pow. 21, 4: 517-524.

[7] Segal C. (2009). Scramjet Engine Process and Characteristics. CAMBRIDGE (ISBN 978-0-521-83815-3).

[8] Chan J et al. (2010). Numerically Simulated Comparative Performance of a Scramjet and Shcramjet at Mach 11. J. Prop. Pow. 26, 5: 1125-1134.

[9] Menees GP et al. (1992). Wave Combustors for Trans-Atmosphericc Vehicles. J. Prop. Pow. 8, 3: 709-713.

[10] Verreault J et al. (2012). Formation and Structure of Steady Oblique and Conical Detonation Waves. AIAA J. 50, 8: 1766-1772.

[11] Maeda S et al. (2012). Oblique detonation wave stability around a spherical projectile by a high time resolution optical observation. Combust. Flame. 159: 887-896.

[12] Vlasenko VV et al. (1995). Numerical Simulation of Inviscid Flows with Hydrogen Combustion Behind Shock Waves and in Detonation Waves. Combust. Explo. Shock Waves. 31, 3: 376-389.

[13] Cambier JL et al. (1990). Numerical Simulation of an Oblique Detonation Wave Engine. Jet Prop. 6, 3: 315-323.

[14] Conaire MO et al. (2004). A comprehensive modeling study of hydrogen oxidation. Int. J. Chem. Kin. 36,11: 603-622.

[15] Yee HC. (1987). Upwind and Symmetric Shock-Capturing Schemes. NASA TM 89464. 159.

[16] Shu CW et al. (1988). Efficient implementation of essentially non-oscillatory shock capturing schemes. J. Comp. Phys. 77, 2: 439-471.

[17] Jameson A et al. (1987). Lower-Upper Implicit Schemes with Multiple Grids for the Euler Equations. AIAA J. 25, 7: 929-935.

[18] Ju Y et al. (1995). Lower-Upper Scheme for Chemically Reacting Flow with Finite Rate Chemistry. AIAA J. 33, 8: 1418-1425.

[19] Lehr HF. (1972). Experiments on Shock-Induced Combustion. Astronaut. Acta. 17: 589-597.

[20] Lee JHS. (2008). The Detonation Phenomenon. CAMBRIDGE (ISBN 978-0-521-89723-5).

[21] Alpert RL et al. (1972). Periodicity in Exothermic Hypersonic Flows about Blunt Projectiles. Astronaut. Acta. 17: 539-560.

[22] Matsuo A et al. (1996). Detailed Mechanism of the Unsteady Combustion Around Hypersonic Projectiles. AIAA J. 34, 10: 2082-2089.